Poly(pyridine)ruthenium(II)-Photoinduced Redox Reactions of Bipyridinium Cations, Poly(pyridine)rhodium Complexes, and Osmium Ammines

Carol Creutz,* Andrew D. Keller, Norman Sutin,* and Arden P. Zipp

Contribution from the Department of Chemistry, Brookhaven National Laboratory, Upton, New York 11973. Received September 11, 1981

Abstract: The quenching of $*RuL_3^{2+}$ (L is a 2,2'-bipyridine or 1,10-phenanthroline derivative) emission by three classes of oxidants Q has been examined. The results are discussed in terms of the Marcus electron-transfer model recast in a preequilibrium formalism. Substituted bipyridinium cations (methyl viologen and related compounds) undergo thermodynamically favorable reduction with a driving force ranging from 0.1 to 0.7 eV and rate constants in the range $(0.4–2.0) \times 10^9 \ M^{-1} \ s^{-1}$, consistent with a diffusion rate constant of $2.0 \times 10^9 \ M^{-1} \ s^{-1}$ and an exchange rate constant of $\sim 10^6 \ M^{-1} \ s^{-1}$ for the $Q–Q^-$ couples. The yields of the separated redox products RuL_3^{3+} and Q^- (typically 0.1 mol einstein^{-1} per quenching act) require k_{30}, the "intramolecular" back-reaction rate constant (to re-form ground-state RuL_3^{2+} and Q), to be $(2–4) \times 10^{10} \ s^{-1}$. Since k_{30} increases weakly with driving force in this series, there is no evidence for inverted behavior despite the fact that $\Delta G°_{30}$ is ~ -2 eV. With $Q = Rh(4,4'-(CH_3)_2bpy)_3^{3+}$, the quenching rate constants, $k_q = (0.001–1.0) \times 10^9 \ M^{-1} \ s^{-1}$, exhibit a great sensitivity to the reducing power of $*RuL_3^{2+}$ and have been fitted to $k_{11} \approx 2 \times 10^9 \ M^{-1} \ s^{-1}$ and $E°_{Q,Q^-} = -0.97$ V for the $RhL_3^{3+}–RhL_3^{2+}$ couple. This $E°$ value is strikingly similar to that (-0.9 V vs. aqueous SCE) obtained via cyclic voltammetry in acetonitrile. The cyclic voltammetry of the RhL_3^{3+} complexes in water has been reexamined, and it is concluded that the irreversibility observed is due to ligand loss from rhodium(I). After correction for an energy transfer component ($k_q = k_{el} + k_{en}$), the rate constants for reduction of $Os^{III}(NH_3)_5X$ ($k_{el} \approx 2 \times 10^6–2 \times 10^8 \ M^{-1} \ s^{-1}$ for X = Cl, Br, I, H_2O, or NH_3) and for oxidation of $Os(NH_3)_5N_2^{2+}$ are in accord with theoretical expectations and osmium(III)–osmium(II) exchange rates in the range $10^2–10^5 \ M^{-1} \ s^{-1}$. Some observations concerning $Os(NH_3)_5Cl^+$, which was generated and characterized by radiation chemistry and flash photolysis techniques, are also reported.

The metal-to-ligand charge-transfer excited state of tris-(2,2'-bipyridine)ruthenium(II)[1-4] has recently found wide application in water photoreduction systems.[1] While $*Ru(bpy)_3^{2+}$ is a sufficiently strong reductant to reduce water to dihydrogen below pH ~ 13,[5,6] the reaction is slow and requires mediators: thus hydrogen formation has been effected by using methyl viologen (MV^{2+} = N,N'-dimethyl-4,4'-bipyridinium cation)[7,8] or Rh-(bpy)$_3^{3+}$[9] as electron shuttles, EDTA or triethanolamine as sacrificial reducing agents, and colloidal platinum as the hydrogen-forming catalyst.[1,7,8]

The formation of hydrogen in the above systems (and in homogeneous systems which have recently been reported[1,10-12]) involves sequences of outer-sphere electron-transfer reactions. The outer-sphere electron-transfer reactivity of MV^{2+} and related bipyridinium derivatives and of Rh(bpy)$_3^{3+}$ and other poly(pyridine)rhodium(III) complexes is thus of considerable interest. In order to probe this reactivity, we have used the series of outer-sphere electron-transfer reagents $*RuL_3^{2+}$, RuL_3^{3+}, and RuL_3^+ where L is a 2,2'-bipyridine or 1,10-phenanthroline derivative. In the past the emphasis has been on using known redox couples to characterize the properties of the $*RuL_3^{2+}–RuL_3^{3+}$, $*RuL_3^{2+}–RuL_3^+$, $RuL_3^{2+}–RuL_3^+$, and $RuL_3^{3+}–RuL_3^{2+}$ couples. These couples are now so well characterized that they may be used to probe the properties of other systems. Because of their great reducing power $*Ru(bpy)_3^{2+}$ and its derivatives are extremely useful for the generation of other highly reducing species (Q^-).

With $*RuL_3^{2+}$, species with potentials as low as -0.9 V may be generated photochemically, while, with its reduction product RuL_3^+, the range may be extended to even lower potentials. Since the reduction potentials of the RuL_3 couples are a function of L, the driving force for redox reactions involving the RuL_3 and $Q–Q^-$ couples may be varied systematically and the free energy dependence of the electron transfer can be ascertained. From such studies, information bearing on the inherent electron-transfer barriers of the $Q–Q^-$ couples may be obtained and, in instances where the reduction potential of the couple cannot be determined by other methods, it may be deduced from the reactivity patterns. This approach has been applied here to bipyridinium cations and to poly(pyridine)rhodium(III) couples. In addition to their importance in hydrogen-forming systems, the bipyridinium cations and their one-electron reduction products are of interest because they, in turn, provide purely organic models for other important bpy–bpy$^-$ couples such as Ru(bpy)$_3^{3+}$–$*Ru(bpy)_3^{2+}$ and Ru-(bpy)$_3^{2+}$–Ru(bpy)$_3^+$. We also describe our experiments with some osmium(III) ammines. Since electrochemical reduction of $Os^{III}(NH_3)_5X$ (X = Cl, Br, I, H_2O, NH_3) has been reported to lead to the reduction of water,[13,14] compounds of this type seemed potential homogeneous hydrogen-formation mediators via a metal–hydride[15] path. Although our efforts to homogeneously mediate water reduction using these compounds were not successful, our chemical and photochemical studies of the osmium complexes led to some results which are of interest in their own right. These systems are discussed in the final section of this paper.

Experimental Section

Materials. Commercial Ru(bpy)$_3Cl_2$·$6H_2O$ (obtained from G. F. Smith Co.) was recrystallized from hot water. The preparation of the other poly(pyridine)ruthenium(II) complexes has been described.[5] The osmium(III) ammines were prepared following the procedures of Buhr and Taube;[16] we are indebted to Dr. Buhr for providing the procedures prior to publication. The method of Allen and Stevens was used for the preparation of pentaamminedinitrogenosmium(II) chloride.[17] The am-

(1) Sutin, N.; Creutz, C. *Pure Appl. Chem.* **1980**, *52*, 2717.
(2) Balzani, V.; Bolletta, F.; Gandolfi, M. T.; Maestri, M. *Top. Curr. Chem.* **1978**, *75*, 1.
(3) Sutin, N. *J. Photochem.* **1979**, *10*, 19.
(4) Whitten, D. G. *Acc. Chem. Res.* **1980**, *13*, 83.
(5) Lin, C.-T.; Böttcher, W.; Chou, M.; Creutz, C.; Sutin, N. *J. Am. Chem. Soc.* **1976**, *98*, 6536.
(6) Sutin, N.; Creutz, C. *Adv. Chem. Ser.* **1978**, *No. 168*, 1.
(7) Moradpour, A.; Amouyal, E.; Keller, P.; Kagan, H. *Nouv. J. Chim.* **1978**, *2*, 547.
(8) Kalyanasundaram, K.; Kiwi, J.; Grätzel, M. *Helv. Chim. Acta* **1978**, *61*, 2720.
(9) Kirch, M.; Lehn, J.-M.; Sauvage, J.-P. *Helv. Chim. Acta* **1979**, *62*, 1345.
(10) Brown, G. M.; Brunschwig, B. S.; Creutz, C.; Endicott, J. F.; Sutin, N. *J. Am. Chem. Soc.* **1979**, *101*, 1298.
(11) Krishnan, C. V.; Sutin, N. *J. Am. Chem. Soc.* **1981**, *103*, 2141.
(12) Brunschwig, B. S.; Sutin, N. *Inorg. Chem.* **1979**, *18*, 1731; *Chem. Phys. Lett.* **1981**, *17*, 63.

(13) Gulens, J.; Page, J. A. *J. Electroanal. Chem. Interfacial Electrochem.* **1974**, *55*, 239.
(14) Gulens, J.; Page, J. A. *J. Electroanal. Chem.* **1976**, *67*, 215.
(15) Malin, J.; Taube, H. *Inorg. Chem.* **1971**, *11*, 2403.
(16) Buhr, J. D.; Winkler, J. R.; Taube, H. *Inorg. Chem.* **1980**, *19*, 2416.
(17) Allen, A. D.; Stevens, J. R. *Can. J. Chem.* **1972**, *50*, 3093.

mines were characterized by comparison of UV–vis and IR spectra with those in the literature[16,17] and by microanalysis. The salt K[Os-(H$_2$EDTA)Cl$_2$]·H$_2$O was prepared and characterized following Saito et al.[18]

The poly(pyridine)rhodium(III) complexes were synthesized by a modification of a literature method;[19] RhCl$_3$·3H$_2$O (1.0 mmol, 0.263 g) dissolved in H$_2$O (10 mL) was warmed with an ethanolic solution (10 mL, 95%) of the poly(pyridine) (3.3 mmol) until the initial precipitate had dissolved, at which point 4 mL of hydrazine hydrate (85%) was added and the solution was refluxed for 24 h. After the solution was cooled, concentrated HClO$_4$ was added dropwise until precipitation was complete. The pink solid (~90% yield) was filtered, washed with water, ethanol, and ether, and then dried in vacuo. In several instances the materials were recrystallized after treatment with activated charcoal[20] to give white solids, but, because this procedure did not alter the analytical or UV spectral properties of the product, but did lower the yield substantially, most of the materials were used without the charcoal treatment. Stock solutions were obtained by slurrying a known weight of solid RhL$_3$(ClO$_4$)$_3$ in water with a small amount of ion-exchange resin (Dowex X8, 100–200 mesh SO$_4^{2-}$ form) until dissolution was complete and then filtering to remove the resin and diluting to volume. In some instances the Rh(III) concentration was determined by X-ray fluorescence to confirm the concentration. Spectra and analyses of the RhL$_3^{3+}$ complexes are given in supplementary Tables I and II.
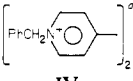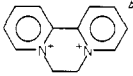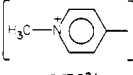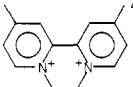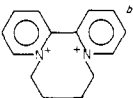
Methyl viologen chloride (*N,N'*-dimethyl-4,4'-bipyridinium chloride, also paraquat) was purchased from Aldrich. The other bipyridinium salts were prepared following literature methods and characterized by their UV spectra.[21]

Fisher-Certified L-ascorbic acid was used in the continuous- and flash-photolysis experiments. Europium(II) solutions were generated by amalgamated zinc reduction of europium(III) solutions.

Methods. Quenching rate constants were obtained from Stern–Volmer plots of emission intensity or emission lifetime data.[5] The quencher concentration ranged from ~3 × 10^{-4} to 5 × 10^{-3} M for the bipyridinium derivatives to 2 × 10^{-2} M for some of the osmium complexes. The RuL$_3^{2+}$ concentration was <10^{-5} M in the emission intensity quenching studies and ~2 × 10^{-5} M in the lifetime studies. Excited-state lifetimes in the absence of quencher (τ_0) were taken from ref 5. The flash-photolysis techniques used to generate and monitor Ru(bpy)$_3^+$ have already been described,[5,22–24] and the conditions used for the osmium(III) complexes are typical: for Os(NH$_3$)$_5$Cl^{2+}, a solution containing 10^{-4} M Ru(bpy)$_3^{2+}$ and 0.03 M Eu(aq)$^{2+}$ in 0.45 M NaCl–0.05 M HCl was excited at 530 nm. The Ru(bpy)$_3^+$ produced through Eu(aq)$^{2+}$ reduction of *Ru(bpy)$_3^{2+}$ was monitored at 490 nm, and its decay was followed as a function of added Os(NH$_3$)$_5$Cl^{2+} (0.5 × 10^{-3}–2.0 × 10^{-3} M). For Os(NH$_3$)$_5$H$_2$O^{3+} and Os(EDTA)$^-$, ascorbate (1.0 M total ascorbate, pH 4–5) was used to reduce *Ru(bpy)$_3^{2+}$ to Ru(bpy)$_3^+$. The pulse radiolysis methods used have been described.[25,26] Continuous-photolysis experiments were carried out on a photolysis train[27] consisting of a 450-W xenon lamp (Christie Corp), cutoff filters and, in some experiments, a Bausch-and-Lomb high-intensity monochromator set to a 20-nm bandpass. Ferrioxalate or Co(NH$_3$)$_5$Cl^{2+} [27] actinometry was used to determine the incident light intensity I_0. Photolysis solutions were thermostated at 25 °C by a circulating water bath and were contained in flat-walled 2 cm^2 by 9-cm high Pyrex bottles.[27] Hydrogen was determined by sampling 0.5–1.0 mL of the ~12-mL gas phase above the 20 mL of solution and injecting onto a molecular sieve column installed in a Perkin-Elmer 154 or a Varian 1400 gas chromatograph with argon as blanket and carrier gas.

Cyclic voltammetric measurements were made with a PAR electrochemistry system consisting of a Model 173 potentiostat and a Model 175 universal programmer and were recorded on an X-Y recorder (BBN Model 850A) at sweep rates between 10 and 500 mV s^{-1} and on an

(18) Saito, M.; Uehiro, T. *Chem. Lett.* **1977**, 809.
(19) Gidney, P. M.; Gillard, R. D.; Heaton, B. T. *J. Chem. Soc., Dalton Trans.* **1972**, 2621.
(20) McKenzie, E. D.; Plowman, R. A. *J. Inorg. Nucl. Chem.* **1970**, *32*, 199.
(21) Homer, R. F.; Tomlinson, T. E. *J. Chem. Soc.* **1960**, 2498.
(22) Creutz, C. *Inorg. Chem.* **1978**, *17*, 1046.
(23) Creutz, C.; Sutin, N.; Brunschwig, B. S. *J. Am. Chem. Soc.* **1979**, *101*, 1297.
(24) Creutz, C.; Chou, M.; Netzel, T. L.; Okumura, M.; Sutin, N. *J. Am. Chem. Soc.* **1980**, *102*, 1309.
(25) Dodson, R. W.; Schwarz, H. A. *J. Phys. Chem.* **1974**, *78*, 892.
(26) Hoselton, M. A.; Lin, C.-T.; Schwarz, H. A.; Sutin, N. *J. Am. Chem. Soc.* **1978**, *100*, 2383.
(27) Chan, S.-F.; Chou, M.; Creutz, C.; Matsubara, T.; Sutin, N. *J. Am. Chem. Soc.* **1981**, *103*, 369. Brown, G. M.; Chan, S.-F.; Creutz, C.; Schwarz, H. A.; Sutin, N. *J. Am. Chem. Soc.* **1979**, *101*, 7638.

Table I. $E_{1/2}$ Values and Rate Constants for the Quenching of *RuL$_3^{2+}$ Emission by Bipyridinium Derivatives at 25 °C in 0.17 M Sodium Sulfate

quencher	$E_{1/2}$, V	10$^{-9}k_q$,[d] M^{-1} s^{-1} L = 5-(Cl)phen	L = bpy	L = 4,7-(CH$_3$)$_2$phen
IV	−0.34	1.86	1.76	2.43
II	−0.38	1.85	2.00	2.40
MV^{2+}	−0.45	1.28	1.18	1.80
I	−0.50	1.46	1.36	2.07
III	−0.65[c]	0.42	0.50	

[a] Prepared as chloride salt. [b] Bromide salt. [c] Reference 29. [d] 5-(Cl)phen is 5-chloro-1,10-phenanthroline; 4,7-(CH$_3$)$_2$phen is 4,7-dimethyl-1,10-phenanthroline.

oscilloscope at greater sweep rates. A conventional H cell was used with a saturated calomel reference (SCE) electrode, a platinum wire auxiliary electrode, and a pyrolytic graphite (aqueous solutions) or platinum (acetonitrile solutions) working electrode. Aqueous solutions were 1–3 mM in RhL$_3^{3+}$ or the bipyridinium derivative and were maintained at 0.5 M ionic strength by the addition of sodium sulfate. Sodium hydroxide was added to the rhodium(III) solutions to a final concentration of 0.05 M. The measurements were made under an argon stream. The acetonitrile solutions were (0.3–0.6) × 10^{-3} M in RhL$_3^{3+}$ and 0.1 M in tetraethylammonium perchlorate (TEAP, Eastman). Acetonitrile (Aldrich Gold Label spectrophotometric grade) was stirred 15 h over P$_2$O$_5$ and distilled under argon before use. The cell was placed in a glovebag filled with dry argon during these measurements. The working platinum electrode was cleaned by immersing it sequentially in concentrated HNO$_3$, water, and 0.1 M TEAP in acetonitrile.

Results

Electrochemical and Quenching Measurements. The results of the cyclic voltammetric measurements performed with the bipyridinium derivatives are presented in Table I. With the exception of III, these cations exhibited clean, reversible behavior on pyrolytic graphite in the aqueous sodium sulfate medium (pH 6 for all but III). The cathodic and anodic peaks exhibited currents of equal magnitude and were separated by ~58 mV at sweep rates (v) of 10–100 mV s^{-1}, with the separation increasing somewhat ($\Delta E_p = (E_{pa} - E_{pc}) = 70$–80 mV) at sweep rates of 200–500 mV s^{-1}. The values of $E_{1/2}$ obtained from the averages of the cathodic and anodic peak potentials (E_{pc} and E_{pa}, respectively) are in excellent agreement with the values reported by other workers.[21,28,29] The strained 2,2'-bpy derivative III has been reported to have $E_{1/2} = -0.65$ V on the basis of polarographic measurements.[29] In our hands III is reduced with E_{pc} values ranging from −0.655 to −0.686 V in the sweep range 10–200 mV s^{-1}, but no oxidation wave was observed under these conditions or even at sweeps as high as 5 V s^{-1}. Similar results were obtained for 10^{-4} and 10^{-3} M III. Values of i_p for the cathodic peak were 25– to

(28) Hunig, S.; Schenk, W. *Liebigs Ann. Chem.* **1979**, 1523.
(29) Amouyal, E.; Zidler, B.; Keller, P.; Moradpour, A. *Chem. Phys. Lett.* **1980**, *74*, 314.
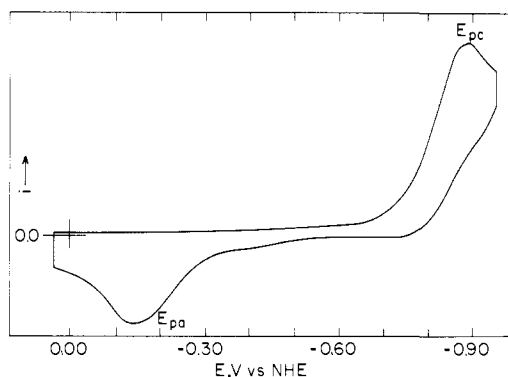
Figure 1. Cyclic voltammogram for Rh[4,4'-(CH₃)₂bpy]₃³⁺ (0.95 × 10⁻³ M in 0.16 M Na₂SO₄, 0.1 M NaOH) at v = 0.2 V s⁻¹.

50% greater than for MV²⁺ with identical concentrations and electrodes. Plots of E_{pc} vs. the natural logarithm of the sweep were linear with slope −0.024 ± 0.004 V. All of the observations made on III in the sodium sulfate, pH 12 medium are consistent with rapid one-electron electrochemical reduction of III followed by a chemical reaction of the reduced species to yield a product which is not electroactive in the −0.2 to −0.7-V region. Since our experiments have not led to an $E_{1/2}$ value for III in the medium used, we shall use the value previously reported in subsequent discussions. The rate constants determined for quenching of emission of RuL₃²⁺ complexes by the five bipyridinium cations are also included in Table I. Values for *Ru(bpy)₃²⁺ quenching by these and other 2,2'-bpy and 4,4'-bpy derivatives have recently been reported under slightly different conditions.[29] The rate constants reported in Table I are 15–50% higher than the latter. These differences probably reflect a medium effect: the present values were obtained in a 0.17 M sulfate (μ = 0.5 M) medium, while the earlier values were found for a ~0.25 M acetate–0.25 M acetic acid (μ = 0.25 M) medium.

The electrochemical behavior of the poly(pyridine)rhodium(III) complexes is extremely complicated as has been noted previously for Rh(bpy)₃³⁺ and Rh(phen)₃³⁺ in both acetonitrile[30] and water as solvents.[27] The behavior shown in Figure 1 for Rh(4,4'-(CH₃)₂bpy)₃³⁺ in aqueous solution is illustrative: the reduction peak seen at ~−0.9 V for this complex is not accompanied by an anodic peak in the same range. Nor is the anodic peak "developed" at rapid (>10 V s⁻¹) sweeps or at low concentrations (<10⁻⁴ M). An anodic wave *is* seen at ~−0.2 V. For Rh(bpy)₃³⁺ the anodic wave was shown to be due to oxidation of Rh(bpy)₂⁺ generated during the cathodic portion of the sweep. The anodic wave in Figure 1 is thus presumably due to the oxidation of Rh(4,4'-(CH₃)₂bpy)₂⁺ and, for the other RhL₃³⁺ complexes, to the oxidation of RhL₂⁺. Since, in this paper, our interest centers on the properties of the RhL₃³⁺–RhL₃²⁺ couples, only parameters relevant to the cathodic peak are considered here. Furthermore, since the behavior of most of the RhL₃³⁺ complexes was similar, we report fairly complete data sets for only three complexes, Rh(5-CH₃phen)₃³⁺, Rh(4,4'-(CH₃)₂bpy)₃³⁺, and Rh(terpy)₂³⁺. These are given in Table II. For 1.0 × 10⁻³ M Rh(bpy)₃³⁺ solutions i_{pc} was found to be 2.7 ± 0.2 times greater than that for 1.0 × 10⁻³ M Cr(bpy)₃³⁺ in the sweep range 1–10 V s⁻¹ on the same electrode.

In contrast to the totally irreversible behavior seen for RhL₃³⁺ in aqueous solution, the first reduction of Rh(bpy)₃³⁺ and related compounds has been seen to exhibit quasi-reversible behavior in acetonitrile at rapid sweep rates.[30] For most of the poly(pyridine)rhodium(III) complexes examined we found behavior analogous to that previously reported: at v ≥ 1 V s⁻¹ an anodic peak accompanied the first reduction peak if the scan direction was reversed rapidly. Table III summarizes the results obtained in acetonitrile. The results obtained in this study for Rh(bpy)₃³⁺ and Rh(phen)₃³⁺ are in reasonably good agreement with those

(30) Kew, G.; DeArmond, K.; Hanck, K. *J. Phys. Chem.* **1974**, *78*, 727. Kew, G.; Hanck, K.; DeArmond, K. *Ibid.* **1975**, *79*, 1829.

Table II. Cyclic Voltammetry of Poly(pyridine)rhodium(III) Complexes on Pyrolytic Graphite in Aqueous Solution (0.1 N Sodium Hydroxide, μ = 0.5 M with Sodium Sulfate) at Room Temperature[a]

complex[b]	v, V s⁻¹	E_{pc},[c] V	i_{pc}, μA	$|E_p - E_{p/2}|$, V
Rh(5-(CH₃)phen)₃³⁺	0.01	−0.846	14.7	0.059
	0.02	−0.854	20.8	0.060
	0.05	−0.866	32.8	0.055
	0.10	−0.877	45.8	0.059
	0.20	−0.886	64.3	0.063
Rh(4,4'-(CH₃)₂bpy)₃³⁺	0.01	−0.850	21.3	0.055
	0.02	−0.861	30.2	0.059
	0.05	−0.871	45.9	0.064
	0.10	−0.881	62.9	0.068
	0.20	−0.891	82.8	0.076
Rh(terpy)₂³⁺	0.01	−0.538	9.4	0.047
	0.02	−0.552	13.2	0.052
	0.05	−0.584	21.2	0.075
	0.10	−0.594	29.6	0.078
	0.20	−0.610	42.8	0.090

[a] The following additional parameters were obtained: i/i_R = 2.2 ± 0.2, and 2.4 ± 0.2 for the 5-(CH₃)phen, 4,4'-(CH₃)bpy, and terpy complexes, respectively. The slope of the linear plot of E_p vs. ln $v^{1/2}$ was 0.0256 and 0.0268 V for the first two complexes, respectively. The ratios i/i_R were obtained by running Cr(bpy)₃³⁺ at the same concentration as the Rh(III) complex on the same electrode. [b] The Rh(III) concentration was 0.91 × 10⁻³, 1.84 × 10⁻³ and 0.47 × 10⁻³ M for the 5-(CH₃)phen, 4,4'-(CH₃)₂bpy, and terpy complexes, respectively. 5-(CH₃)phen is 5-methyl-1,10-phenanthroline; 4,4'-(CH₃)₂bpy is 4,4'-dimethyl-2,2'-bipyridine; terpy is 2,2',2''-terpyridine. [c] The reproducibility of the E_{pc} (cathodic peak potential) values on various solutions and electrodes was ±10 mV.

in the literature[30] ($E_{1/2}$ = −0.83 and −0.75 V, respectively). Values of E_{pc} obtained in aqueous solution on a pyrolytic graphite electrode at v = 0.02 V s⁻¹ are also given in Table III for comparison.

Rate constants for the quenching of the *RuL₃²⁺ emission by poly(pyridine)rhodium(III) complexes are summarized in Table IV.

Rate constants for the quenching of the *RuL₃²⁺ emission by osmium(II) and -(III) complexes, along with potentials reported[13,14] for the Os(III)–Os(II) couples are presented in Table V.

Continuous Photolysis. Continuous photolysis of bipyridinium cation–Ru(bpy)₃²⁺ solutions (4 × 10⁻⁶ M Ru(bpy)₃²⁺, 2 × 10⁻³ M bipyridine cation, 0.02 M triethanolamine, pH 8.1, 0.5 M ionic strength with sodium sulfate) with 450 ± 20-nm light yielded the colored bipyridine radical ions. The quantum yields for the formation of the radical ions were determined by assaying the reduced species spectrophotometrically. After correction for the fraction not quenched,[27] the yields ϕ are as follows (ϵ_{max}, λ_{max}): MV⁺, 0.25[27] (1.24 × 10⁴ M⁻¹ cm⁻¹ at 602 nm[31]); I⁻, 0.1 (0.29 × 10⁴ M⁻¹ cm⁻¹ at 737 nm); II⁻, 0.2 (0.20 × 10⁴ M⁻¹ cm⁻¹ at 740 nm); IV⁻, 0.17 (1.01 × 10⁴ M⁻¹ cm⁻¹ at 598 nm[31]).

Continuous photolysis of Ru(bpy)₃²⁺–osmium(III) solutions under a range of conditions produced no significant yield of H₂ as is shown in Table VI.

Flash Photolysis. No redox products were detected for the quenching of *Ru(bpy)₃²⁺ by Os(NH₃)₅I²⁺, for the quenching of *Ru(bpy)₃²⁺ and *Ru(4,7-(CH₃)₂phen)₃²⁺ by Os(NH₃)₅H₂O³⁺ or Os(NH₃)₅Cl²⁺, or for the quenching of *Ru(bpy)₃²⁺ by Os^III(EDTA)⁻. The observations impose an upper limit of ~0.05 on the cage escape yield of Ru(III) and Os(II) or of RuL₃⁺ and Os(IV) per quenching act. Rate constants obtained for oxidation of Ru(bpy)₃⁺ photogenerated by Eu²⁺ reduction (method A) or ascorbate reduction (method B) at 25 °C and 0.5 M ionic strength are as follows: MV²⁺, 1.6 × 10⁹ M⁻¹ s⁻¹ (B); Rh(4,4'-(CH₃)₂bpy)₃³⁺, 3.7 × 10⁹ M⁻¹ s⁻¹ (B); Os(NH₃)₅Cl²⁺, 1.0 × 10⁹ M⁻¹ s⁻¹ (A); Os(EDTA)⁻, 1.1 × 10⁹ M⁻¹ s⁻¹ (B). The rate constant for the oxidation of MV⁺ by ascorbate radical at pH 4 and 0.5

(31) Steckhan, E.; Kuwana, T. *Ber. Bunsenges. Phys. Chem.* **1974**, *78*, 253.

Table III. Cyclic Voltammetry of Poly(pyridine)rhodium(III) Complexes on a Platinum Electrode in 0.1 M Tetraethylammonium Perchlorate–Acetonitrile at Room Temperature

complex[b]	$(-E_{pc}{}^{aq})$,[a] V	v, mV s^{-1}	I $-E_{pc}$,[b] V	I $E_{pc}-E_{pa}$,[c] V	II $-E_{pc}$,[b] V
Rh(terpy)$_2{}^{3+}$	(0.55)	1	0.66	0.10	0.85
		2	0.70		0.87
		5	0.72		
		10	0.80		
Rh(bpy)$_3{}^{3+}$	(0.75	1	0.83	0.05	
		2	0.84	0.07	$(\sim0.96)^d$
		5	0.85	0.09	$(\sim0.97)^d$
		10	0.86	0.11	
Rh(4,4'-(CH$_3$)$_2$bpy)$_3{}^{3+}$	(0.86)	1	0.93	0.06	
		2	0.94	0.08	
		5	0.95	0.10	1.10
		10			1.12
Rh(5-(Cl)phen)$_3{}^{3+}$	(0.64)	1	0.72	. . .	0.97
		2	0.72	0.08	0.99
		5	0.73	0.11	1.04
Rh(5-(Br)phen)$_3{}^{3+}$	(0.62)	2	0.73	. . .	
		5	0.74	0.08	0.93
		10	0.75	0.09	
Rh(phen)$_3{}^{3+}$	(0.71)	1	0.80	0.06	
		2	0.81	0.07	1.06
		5	0.82	0.09	1.06
		20	0.84	0.11	
		50	0.86	0.14	
Rh(5-(Ph)phen)$_3{}^{3+}$	. . .	1	0.82	0.07	1.00
		2	0.83	0.09	1.03
		5	0.84	0.11	
Rh(5-(CH$_3$)phen)$_3{}^{3+}$	(0.85)	1	0.84	0.07	
		2	0.85	0.08	
		5	0.86	0.09	1.08
		10	0.87	0.10	
		20	0.88	0.12	
Rh(5,6-(CH$_3$)$_2$phen)$_3{}^{3+}$	(0.83)	1	0.88	0.07	1.05
		2	0.89	0.08	1.06
		5	0.90	0.10	
Rh(4,7-(CH$_3$)$_2$phen)$_3{}^{3+}$	(0.80)	1	0.96	0.06	1.19
		2	0.97	0.08	1.20
		5	0.97	0.08	1.21
		10	0.98	0.10	
		20	0.99	0.11	1.20
		50	1.04	0.17	1.25
		100	1.08	0.23	1.28

^{a} Potential vs. SHE. These E_{pc} values were obtained at 20 mV s^{-1} sweep rate in *aqueous* 0.05 M NaOH and 0.15 M Na$_2$SO$_4$. ^{b} Potential vs. aqueous SCE. ^{c} Obtained when scan direction was reversed $\sim$0.1 V cathodic of E_{pc}. ^{d} Shoulder on peak I, not well resolved.

Table IV. Rate Constants for the Quenching of *RuL$_3{}^{2+}$ Emission by RhL$_3{}^{3+}$ Complexes in Aqueous Solutions at 25 °C and 0.5 M Ionic Strength[a]

RhL$_3{}^{3+}$, L	$10^{-9}k_q$, M^{-1} s^{-1}, for *RuL$_3{}^{2+}$, L 5-(Cl)phen	bpy	phen	5-(CH$_3$)phen	4,7-(CH$_3$)$_2$phen
5-(Br)phen		1.5			
5-(Cl)phen		1.5			
5-(Ph)phen		1.6			
phen		0.4			
bpy	0.21	0.6	0.6	0.7	0.9
4,7-(CH$_3$)$_2$phen		1.73			
5,6-(CH$_3$)$_2$phen		0.3	0.95	1.3	1.6
5-(CH$_3$)phen	0.16	0.4	0.98	1.0	1.3
4,4'-(CH$_3$)$_2$bpy	0.001	0.03	0.2	0.49	1.2

^{a} The k_q values were obtained in 0.17 M Na$_2$SO$_4$.

M ionic strength was found to be $\sim$2 × 10^8 M^{-1} s^{-1} (B, MV^{2+} = 5 × 10^{-5} M).

Pulse-Radiolysis Experiments. Argon-scrubbed solutions 10^{-4} M in Os(NH$_3$)$_5$Cl^{2+} and 0.1 M in *tert*-butyl alcohol were subjected to 1–4-μs pulses of 2-MeV electrons produced in a Van de Graaff and monitored in the ultraviolet region. The reaction of Os-(NH$_3$)$_5$Cl^{2+} with both hydrated electrons (pH 4.8, acetate buffer) and hydrogen atoms (pH 2, CF$_3$SO$_3$H) was very rapid; at 25 °C and 0.01 M ionic strength the rate constants were $\gg$5 × 10^9 and

$\sim$5 × 10^9 M^{-1} s^{-1}, respectively. The difference spectrum of the reduction product had a maximum at 305 nm and a shoulder at $\sim$360 nm. Higher values of G_ϵ (2100 and 1100 M^{-1} cm^{-1} at 360 and 305 nm, respectively, where G = yield of product per 100 eV absorbed) were obtained at pH 5 than at pH 2 (1100 and 700 M^{-1} cm^{-1}) presumably because H atom recombination lowers the Os(II) yield at pH 2. This was confirmed by the fact that G_ϵ values increased somewhat at higher Os(III) at pH 2. At pH 3 and 5 about half the transient absorbance decayed within 4 ms. The decays were wavelength dependent and nonexponential. At pH 2, however, good first-order decays with k_{obsd} = (5.5 ± 1.1) × 10^2 s^{-1} independent of dose and osmium(III) concentration ((1–5) × 10^{-4} M) were obtained. The transient Os(NH$_3$)$_5$Cl$^+$ decayed to a product which (like Os(NH$_3$)$_5$Cl^{2+}) does not absorb significantly at λ > 300 nm. At shorter wavelengths the absorbance was somewhat less after the decay reaction than before the pulse.

Continuous-radiolysis experiments showed that very little hydrogen is formed in the decomposition of Os(NH$_3$)$_5$Cl$^+$. γ-Irradiation (2000 Ci ^{60}Co source) of solutions 0.1 M in *tert*-butyl alcohol and 1.0 × 10^{-4} M in Os(NH$_3$)$_5$Cl^{2+} adjusted to pH 4 and 2 yielded H$_2$ with G = 0.55 and 1.1, respectively, as determined by gas chromatography of the solution. The spectra of the solutions after extensive radiolysis was virtually unaltered; after 65-min exposure to the ^{60}Co source the Os(NH$_3$)$_5$Cl^{2+} absorption diminished $\sim$10% uniformly between 200 and 400 nm (G for disappearance of Os(NH$_3$)$_5$Cl^{2+} $\sim$0.05).

Table V. Rate Constants for the Quenching of $*RuL_3^{2+}$ Emission by Osmium(II) and Osmium(III) Ammine Complexes at 25 °C in 0.5 M Sulfuric Acid

	$10^{-8}k_q$, M^{-1} s^{-1}				
L^a	$Os(NH_3)_5N_2^{2+}$ $E° = +0.56$ V^b	$Os(NH_3)_5Cl^{2+}$ $E° = -0.85$ V^c	$Os(NH_3)_6^{3+}$ $E° = -0.78$ V^c	$Os(NH_3)_5I^{2+}$ $E° = -0.77$ V^c	$Os(NH_3)_5(H_2O)^{3+}$ $E° = -0.73$ V^c
5-(Cl)phen	5.2	≤0.2	≤0.09	3.2	≤0.05
bpy	0.9	≤0.4	≤0.14	3.2	≤0.07
5,6-$(CH_3)_2$phen			≤0.3	6.6	≤0.2
4,7-$(CH_3)_2$phen	≤0.3	3.0	0.50		0.87
3,5,6,8-$(CH_3)_4$phen				6.6	0.49
3,4,7,8-$(CH_3)_4$phen		4.2	0.79	8.5	1.4

^{a} Abbreviations used: 5-(Cl)phen, 5-chloro-1,10-phenanthroline; bpy, 2,2'-bipyridine; 5,6-$(CH_3)_2$phen, 5,6-dimethyl-1,10-phenanthroline; 4,7-$(CH_3)_2$phen, 4,7-dimethyl-1,10-phenanthroline; 3,5,6,8-$(CH_3)_4$phen, 3,5,6,8-tetramethyl-1,10-phenanthroline; 3,4,7,8-$(CH_3)_4$phen, 3,4,7,8-tetramethyl-1,10-phenanthroline. ^{b} From ref 16. ^{c} From ref 13 and 14, determined at 0.3 M ionic strength.
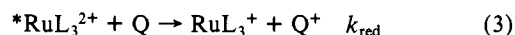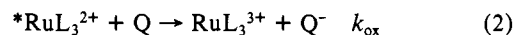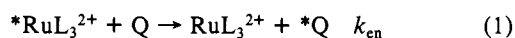
Table VI. Yields of Hydrogen Obtained at 25 °C with Irradiation at 450 ± 20 nm and Light Intensity ~6 × 10^{-8} einstein cm^{-2} s^{-1} ^{a}

| reductant	medium	[Os(III)]	μL of H_2/min	$\phi(H_2)$, mol einstein^{-1}
0.1 M $Eu(aq)^{2+}$	1 M HTFA^b	1.8×10^{-3} M $Os(NH_3)_5Cl^{2+}$	0.05	≤10^{-3} ^{c}
0.1 M $Eu(aq)^{2+}$	1 M HTFA^b	none	1.5	g
0.9 M HA$^{-d,e}$	$H_2A + HA^- = 1.0$ $M,^e$ pH 5	1.0×10^{-3} M $Os(NH_3)_5Cl^{2+}$	<0.02	<<10^{-3}
0.05 M $Eu(aq)^{2+}$	1 M HCl	1.0×10^{-3} M $Os(EDTA)^-$	200^f	f
0.05 M $Eu(aq)^{2+}$	1 M HCl	none	1.4	g
0.45 M HA^{-e}	$H_2A + HA^- = 0.50$ M, pH 5	1.0×10^{-3} M $Os(EDTA)^-$	≤0.05	≤10^{-3}
0.5 M HA^{-h}	$H_2A + HA^- = 1.0$ M, pH 4.1	2.0×10^{-3} M $Os(NH_3)_5Cl^{2+}$		0.8×10^{-4}
0.08 M HA^{-h}	$H_2A + HA^- = 1.0$ M, pH 3.0	2.0×10^{-3} M $Os(NH_3)_5Cl^{2+}$		<<10^{-3}

^{a} A 20-mL sample of solution below a ~10-mL gas space was irradiated for 30 min. The concentration of $Ru(bpy)_3^{2+}$ was 1.0×10^{-4} M unless otherwise stated. ^{b} HTFA is trifluoroacetic acid; $Os(NH_3)_5Cl^{2+}$ is not soluble in HCl. ^{c} Note that more H_2 is formed in the absence than in the presence of $Os(NH_3)_5Cl^{2+}$. ^{d} 0.4×10^{-4} M $Ru(bpy)_3^{2+}$. ^{e} The abbreviations HA$^-$ and H_2A are used for ascorbate ion and ascorbic acid. Ascorbate ion is present as the sodium salt. ^{f} This high rate of H_2 formation is not a consequence of a simple photochemical process. Note that under these conditions $Os(EDTA)^-$, rather than $Eu^{2+}(aq)$, is the quencher. The H_2 formation exhibits an induction period (the rate given is the one observed after the induction period), and H_2 evolution at a comparable rate continues in the dark after the induction period. ^{g} These rates have not been corrected for the H_2 evolution which occurs in the dark. ^{h} 5×10^{-4} M $Ru(bpy)_3^{2+}$; $I_0 = 10^{-6}$ einstein s^{-1}.

Discussion

Three bimolecular processes leading to the quenching of the luminescent metal-to-ligand charge-transfer excited states of poly(pyridine)ruthenium(II) complexes have been elucidated[1-6] and are summarized in eq 1-3. The energy-transfer process (eq

$$*RuL_3^{2+} + Q \rightarrow RuL_3^{2+} + *Q \qquad k_{en} \qquad (1)$$

$$*RuL_3^{2+} + Q \rightarrow RuL_3^{3+} + Q^- \qquad k_{ox} \qquad (2)$$

$$*RuL_3^{2+} + Q \rightarrow RuL_3^+ + Q^+ \qquad k_{red} \qquad (3)$$

1) leads to deactivation of $*RuL_3^{2+}$ and concomitant formation of excited quencher; its rapidity is determined by the overlap of the $*RuL_3^{2+}$ emission and Q absorption spectra, among other factors.[24] Rate constants for quenching of $*RuL_3^{2+}$ by chromium(III) complexes via an energy-transfer mode have been found to vary little with L.[5] This is not unexpected since the excitation energies and spectra of the RuL_3^{2+} complexes do not show much dependence on L. By contrast, very large variations in the magnitudes of the quenching rate constants may be obtained when the quenching involves oxidation (eq 2) or reduction (eq 3) of the excited state. For the most part, the quenching processes documented for $*RuL_3^{2+}$ have involved outer-sphere electron-transfer reactions. As in the outer-sphere electron-transfer reactions of ground states, the redox quenching rate constants increase with driving force and the rate variations with changing L arise because the redox potential of $*RuL_3^{2+}$ is a function of L. The reduction potential $*E°_{3,2}$ (eq 4) relevant to the oxidative quenching process

$$RuL_3^{3+} + e^- = *RuL_3^{2+} \quad *E°_{3,2} \qquad (4)$$

$$*RuL_3^{2+} + e^- = RuL_3^+ \quad *E°_{2,1} \qquad (5)$$
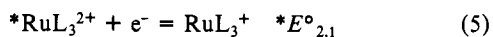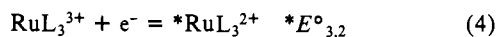
Scheme I
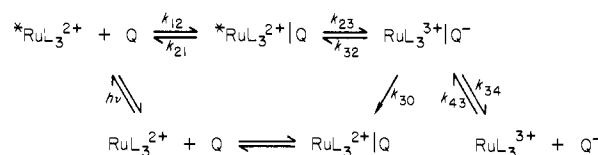
(eq 2) ranges from ~−0.7 to ~−0.9 V in the substituted bpy and phen series.[5] Similarly, the reduction potential $*E°_{2,1}$ (eq 5) relevant to reductive quenching (eq 3) spans the range +0.7 to +1 V.[6,22] Additional factors which determine the magnitude of k_q for redox quenching include the reduction potential of the Q^+–Q or Q–Q$^-$ couple and the intrinsic electron-transfer barriers of the quencher and $*RuL_3^{2+}$ couples. As has been discussed elsewhere, the $*RuL_3^{2+}$–RuL_3^{3+} and RuL_3^+–$*RuL_3^{2+}$ couples feature only very small electron-transfer barriers. In fact, self-exchange rate constants of ≥10^8 and ~10^9 M^{-1} s^{-1} have been estimated for eq 6 and 7, respectively.[1]

$$*RuL_3^{2+} + RuL_3^{3+} \rightleftharpoons RuL_3^{3+} + *RuL_3^{2+} \qquad (6)$$

$$RuL_3^+ + *RuL_3^{2+} \rightleftharpoons *RuL_3^{2+} + RuL_3^+ \qquad (7)$$

With the above as background, we consider the detailed quenching mechanism. This is shown in Scheme I for oxidative quenching. The reactants diffuse together to give a precursor complex. "Intramolecular" electron transfer within the precursor complex yields the successor complex in which RuL_3^{3+} and Q^- remain in close proximity within the solvent cage. Dissociation of the successor complex yields the separated electron-transfer products; electron back-transfer within the successor complex yields ground state RuL_3^{2+} and Q. Use of the steady-state ap-

Poly(pyridine)ruthenium Redox Reactions

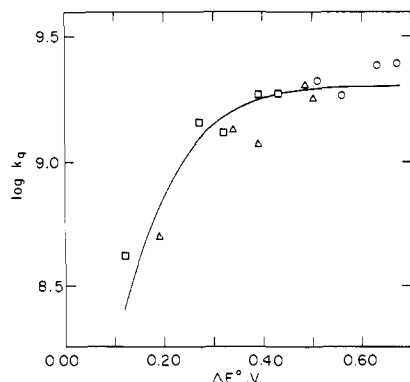*J. Am. Chem. Soc., Vol. 104, No. 13, 1982* 3623

Figure 2. The logarithm of the rate constant for quenching of $*RuL_3^{2+}$ emission by bipyridinium derivatives vs. the logarithm of the equilibrium constant for electron transfer from $*RuL_3^{2+}$. The curve was calculated by using the following parameters and eq 10: $k_{11}k_{22} = 1 \times 10^{15}$ M^{-2} s^{-2}, $\kappa = 1$, $K\nu = 2 \times 10^{12}$ M^{-1} s^{-1}, diffusion rate constant 2.0×10^9 M^{-1} s^{-1}. The RuL_3^{2+} complexes used were L = $4,7-(CH_3)_2$phen (circles), L = bpy (triangles), and L = 5-(Cl)phen (squares).

proximation for the concentrations of the precursor and successor complexes yields the following expression for the quenching rate constant[32]

$$k_q = \frac{K_{12}k_{23}}{1 + K_{12}k_{23}/k_{12} + k_{32}/(k_{30} + k_{34})} \quad (8)$$

where $K_{12} = k_{12}/k_{21}$ is the equilibrium constant for the formation of the precursor complex. For many purposes it is convenient to introduce a diffusion-corrected quenching rate constant k_{qc} defined by

$$\frac{1}{k_{qc}} = \frac{1}{k_q} - \frac{1}{k_{diff}}$$

where $k_{diff} = k_{12}$ is the rate constant for diffusion together of the two reactants. Thus for Scheme I k_{qc} is given by

$$k_{qc} = \frac{K_{12}k_{23}}{1 + k_{32}/(k_{30} + k_{34})} \quad (9)$$

The cage escape yield (the yield of separated products) derives from competition between the dissociation of the successor complex and electron back-transfer to yield RuL_3^{2+} and Q. It is given by $\phi_{cage} = k_{34}/(k_{30} + k_{34})$. Even after the redox products escape the solvent cage they may diffuse together again and so undergo back-reaction with a second-order rate constant $k_t = k_{43}k_{30}/(k_{30} + k_{34})$. Similar parameters thus determine the initial yields of redox products and the rates of their ultimate destruction.

We now turn to the behavior of the individual systems.

Bipyridinium Cations. The quenching of $*Ru(bpy)_3^{2+}$ emission by methyl viologen and analogous compounds has been attributed to an oxidative quenching process (eq 2); indeed the colored radical MV^+ has been observed in both flash- and continuous-photolysis experiments.[29,33,34] The quenching rate constants in Table I are thus identified with k_{ox} in eq 2. As expected for oxidative quenching, these k_q values increase with log K_{23} ($=16.9(E^\circ_{Q-Q^-} - *E^\circ_{2,3})$). The range in k_q ($(0.4-2.4) \times 10^9$ M^{-1} s^{-1}) is small, but this is a result of the fact that, at large K_{23}, the values become diffusion limited.

Because the quenching of $*RuL_3^{2+}$ by the bipyridinium cations is exothermic, $k_{34} \gg k_{32}$, and the reverse of the quenching step can be neglected. Under these conditions eq 8 and 9 reduce to eq 10a and 10b, respectively. In Figure 2 a plot of log k_q vs. ΔE°

$$k_q = \frac{K_{12}k_{23}}{1 + K_{12}k_{23}/k_{12}} \quad (10a)$$

$$k_{qc} = K_{12}k_{23} \quad (10b)$$

for the data in Table I is shown. The curve is calculated from eq 10 by using $k_{12} = k_{diff} = 2.0 \times 10^9$ M^{-1} s^{-1}, and k_{12} and k_{23} are given by[35]

$$K_{12} = \frac{4\pi N r^2 \delta r}{1000} \exp(-w/RT) \quad (11)$$

$$k_{23} = \nu_{23}\kappa_{23} \exp(-\Delta G^*_{23}/RT) \quad (12)$$

$$\Delta G^*_{23} = (\Delta G^*_0)_{23}\left[1 + \frac{\Delta G^\circ_{23}}{4(\Delta G^*_0)_{23}}\right]^2 \quad (13)$$

In the above equations r is the separation of the centers of the two reactants, δr is the thickness of the reaction layer (~ 1 Å), w is the work required to bring the two reactants together, ν_{23} is a nuclear frequency factor, κ_{23} is the electronic factor for the reaction (in the normal free energy region $\kappa = 1$ for an adiabatic reaction; $\kappa \ll 1$ for a nonadiabatic reaction), and the reorganization free energy at zero driving force $(\Delta G^*_0)_{23}$ is given by

$$(\Delta G^*_0)_{23} = (\Delta G^*_{11} + \Delta G^*_{22})/2$$

where ΔG^*_{11} and ΔG^*_{22} are the reorganization free energies (self-exchange rate constants k_{11} and k_{22}) of the two couples involved in the quenching reaction. In the present calculations the work terms have been neglected, κ was assumed equal to unity, $K\nu = 2 \times 10^{12}$ M^{-1} s^{-1} and $\Delta G^*_0 = 0.284$ eV, corresponding to $k_{11}k_{22} = 1.0 \times 10^{15}$ M^{-2} s^{-2}, were used.[37] The agreement of the calculated and observed free energies of activation is seen to be satisfactory.

Bock et al. have carried out a similar study of bipyridinium cation quenching in acetonitrile and fitted the free energy dependence with $k_{diff} = 3 \times 10^{10}$ M^{-1} s^{-1} and $k_{11}k_{22} = 2.8 \times 10^{15}$ M^{-2} s^{-2}.[38] The data of Amouyal et al.,[29] obtained for aqueous solutions, were fitted with $k_{diff} = 3 \times 10^9$ M^{-1} s^{-1} and $k_{11}k_{22} = 10^{14}$ M^{-2} s^{-2}. The three studies (considering differences in media and solvent) thus give reasonably consistent parameters. The most striking result is the small magnitude of $k_{11}k_{22}$ $((0.1-2.8) \times 10^{15}$ M^{-2} $s^{-2})$ implied by the three studies. The $*Ru(bpy)_3^{2+}-Ru(bpy)_3^{3+}$ exchange rate constant has been estimated as $(0.5-2.0) \times 10^9$ M^{-1} s^{-1} so that the Q^--Q exchange rate constant lies in the range $(0.5-2.0) \times 10^6$ M^{-1} s^{-1} under the present conditions. The Q^--Q exchanges are thus appreciably slower than the $*Ru(bpy)_3^{2+}-Ru(bpy)_3^{3+}$ exchange. Both exchanges involve transfer of an electron from the π^* orbital of a pyridine ring to the π^* orbital of another pyridine ring. Both MV^{2+} and IV are $4,4'$-bpy derivatives, but (like $Ru(bpy)_3$) the other three compounds in Table I are $2,2'$-bpy derivatives; $C_2H_4^{2+}$ or $C_4H_8^{2+}$ replaces the Ru(II) or Ru(III) metal center. Because of efficient overlap of the π^* orbitals on the electron donor and acceptor, the $*Ru(bpy)_3^{2+}-Ru(bpy)_3^{3+}$ and Q^--Q exchanges, as well as the $*Ru(bpy)_3^{2+}-Q$ cross-reactions, are very like to be adiabatic (κ for the k_{23} step ~ 1). The inner-shell reorganization barriers are probably also very small for these processes because the distortions

(32) Rehm, D.; Weller, A. *Ber. Bunsenges. Phys. Chem.* **1969**, *73*, 834; *Isr. J. Chem.* **1970**, *8*, 259.

(33) Bock, C. R.; Whitten, D. G.; Meyer, T. J. *J. Am. Chem. Soc.* **1974**, *96*, 4710.

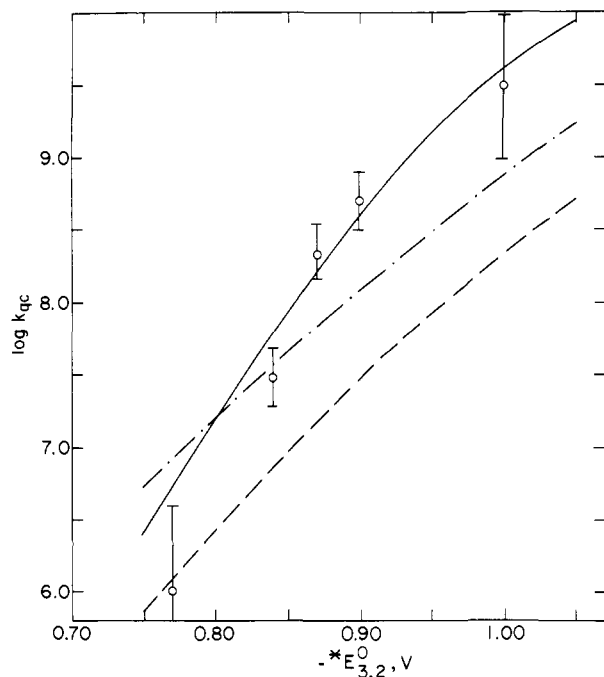(34) Kalyanasundaram, K.; Kiwi, J.; Grätzel, M. *Helv. Chim. Acta* **1978**, *61*, 2720.

(35) (a) Sutin, N.; Brunschwig, B. S. *Adv. Chem. Ser.*, in press. Sutin, N. "Inorganic Reactions and Methods"; Zuckerman, J. J., Ed.; Verlag Chemie: Weinheim/Bergstr., Germany; Sections 12.2.3 and 13.4, in press. (b) Marcus, R. A. *Annu. Rev. Phys. Chem.* **1964**, *15*, 155; *J. Chem. Phys.* **1965**, *43*, 679.

(36) Creutz, C.; Kroger, P.; Matsubara, T.; Netzel, T. L.; Sutin, N. *J. Am. Chem. Soc.* **1979**, *101*, 5442.

(37) In principle the choice of the parameters used to fit data such as those in Figure 2 is determined by one data point and eq 12: the value of log k_{qc} at $\Delta E^\circ = 0$ is equal to (log $k_{11}k_{22})/2$; at this point the slope of the log k_{qc} vs. ΔE° plot is equal to 8.5. The slope decreases with increasing ΔE° with a curvature proportional to log $k_{11}k_{22}$. Thus, if ΔE° is known, then the value of (log $k_{11}k_{22})/2$ is uniquely determined by the value of log k_{qc} at $\Delta E^\circ = 0$; if ΔE° is not known, then (log $k_{11}k_{22})/2$ (and $\Delta E^\circ = 0$) occurs at the slope of 8.5 in the plot of log k_{qc} vs. $*E^\circ$ (or E°_Q). In general the fitting procedure is an iterative one. Depending upon the system, the above procedure may give the best initial set of trial parameters. However when ΔE° is not known (as for the RhL_3^{3+} data) and use of the full eq 14 is required, extrapolation of data for the endergonic region (slope $\gg 8.5$) as described in ref 38 readily provides a good trial value of ΔE°.

(38) Bock, C. R.; Connor, J. A.; Gutierrez, A. R.; Meyer, T. J.; Whitten, D. G.; Sullivan, B. P.; Nagle, J. K. *J. Am. Chem. Soc.* **1979**, *101*, 4815.

Figure 3. The logarithm of the diffusion-corrected rate constant for the quenching of *RuL$_3^{2+}$ emission by Rh[4,4'-(CH$_3$)$_2$bpy]$_3^{3+}$ vs. the reduction potential for the RuL$_3^{3+}$–*RuL$_3^{2+}$ couple. The solid curve was calculated from eq 14 using the following parameters: $E°_{Q,Q^-}$ = −0.97 V; $k_{11}k_{22}$ = 5.25 × 10^{18} M^{-2} s^{-2} (ΔG_0^* = 0.209 eV); ν_{23} = 1 × 10^{13} s^{-1}; k_{30} = 1.7 × 10^{10} s^{-1}; K_{12} = 0.7 M^{-1}; diffusion rate constant 2.0 × 10^9 M^{-1} s^{-1}. For comparison, the dashed curve was calculated by using $E°_{Q,Q^-}$ = −0.97 V and $k_{11}k_{22}$ = 1 × 10^{16} M^{-2} s^{-2} (ΔG_0^* = 0.290 eV) and the dashed-dot curve calculated by using $E°_{Q,Q^-}$ = −0.89 V and $k_{11}k_{22}$ = 1 × 10^{16} M^{-2} s^{-2}.

are spread over many bonds. The most likely source of the relative "slowness" of the Q$^-$–Q exchanges is an increased solvent (outer-shell) barrier to the electron transfer arising from the smaller effective radii of the reactants.

Detailed continuous photolysis studies of the Ru(bpy)$_3^{2+}$, MV^{2+}, and triethanolamine (TEOA) system have shown that the quantum yield for MV$^+$ formation (ϕ_{Q^-}) at pH 8 is twice the cage escape yield.[27] (A second MV$^+$ is produced by the reduction of MV^{2+} by a TEOA radical.[27,34]) Here we have assumed the same behavior for the other bipyridinium cations and have used ϕ_{Q^-} to estimate ϕ_{cage} = 0.5 ϕ_{Q^-}. The quantity [(ϕ_{cage})$^{-1}$ − 1] is equal to k_{30}/k_{34}. If k_{34} is taken as 2.0 × 10^9 s^{-1} (equivalent to taking K_{43} as 1.0 M^{-1}), then values of the first-order electron-transfer rate constant for reaction of RuL$_3^{3+}$ with Q$^-$ can be calculated. These are as follows (Q, $\Delta E°$, k_{30}): I, 1.76 V, 3.8 × 10^{10} s^{-1}; MV^{2+}, 1.71 V, 1.4 × 10^{10} s^{-1}; II, 1.64 V, 1.8 × 10^{10} s^{-1}; IV, 1.60 V, 2.4 × 10^{10} s^{-1}. The rate constants are seen to be essentially independent of $\Delta E°$. Moreover, even the largest value obtained is about 100 times smaller than the maximum rate constant ($\nu \approx 10^{13}$ s^{-1}) possible. This suggests that the relatively large cage escape yields (and low k_{30} values) for the RuL$_3^{3+}$–Q$^-$ reactions result from nonadiabaticity (κ for the k_{30} step 10^{-2}–10^{-3}) and/or from control of the reaction by the relatively slow solvent reorganization.[36] The k_{30} estimates obtained here (2–4) × 10^{10} s^{-1} may be compared with 5 × 10^{10} s^{-1} estimated by Bock et al.[38] for the analogous reactions in acetonitrile. Finally, our finding that k_{30} does not decrease with increasing driving force is an important result: it is at variance with the requirements of existing classical (and quantum mechanical) models that predict a decrease in rate constant with increasing driving force when $\Delta G° < -4\Delta G^*_0$.

Rhodium(III) Poly(pyridine) Complexes. Flash-photolysis studies of the *Ru(bpy)$_3^{2+}$–Rh(bpy)$_3^{3+}$ system have confirmed that quenching of *Ru(bpy)$_3^{2+}$ proceeds by eq 2.[27] In agreement, the k_q values in Table IV generally increase across a row (*$E°_{3,2}$ decreases from left to right). This trend is more readily apparent in Figure 3 in which log k_{qc} for quenching by Rh(4,4'-(CH$_3$)$_2$bpy)$_3^{3+}$ is plotted against *$E°_{3,2}$ for the RuL$_3^{3+}$–*RuL$_3^{2+}$

Table VII. Reduction Potentials of Poly(pyridine)rhodium(III) and -ruthenium(III) Complexes at Room Temperature

L	RhL$_3^{3+}$–RhL$_3^{2+}$		RuL$_3^{3+}$–*RuL$_3^{2+}$
	$E_{1/2}$(CH$_3$CN),[a] V	$E°_{Q-Q^-}$,[b] V	*$E°_{3,2}$,[b,c] V
bpy	−0.81	−0.86	−0.84
4,4'-(CH$_3$)$_2$bpy	−0.90	−0.97	−0.94
5-(Cl)phen	−0.68		−0.77
5-(Br)phen	−0.70		−0.76
phen	−0.77	−0.84	−0.87
5-(Ph)phen	−0.79		−0.87
5-(CH$_3$)phen	−0.81	−0.88	−0.90
5,6-(CH$_3$)$_2$phen	−0.85	−0.89	−0.93
4,7-(CH$_3$)$_2$phen	−0.93		−1.01

[a] Potential vs. SCE in acetonitrile. [b] Potential vs. SHE in water. [c] From ref 5.

couple. (In contrast to Figure 2 where the abscissa is $\Delta E°$, here only the *relative* driving force is used since the $E°$ for the RhL$_3^{3+}$–RhL$_3^{2+}$ couples has not been directly measured in water.) Two features of the data are striking: first, the "slope" for the first four points is much greater than the 8.5 V^{-1} expected for moderately exothermic electron transfer but is close to that (∼16.9 V^{-1}) expected for endergonic electron transfer. Secondly, the steep slope continues into a region of very high k_q, suggesting that the intrinsic barrier to electron transfer from *RuL$_3^{2+}$ to RhL$_3^{3+}$ is quite small. In order to fit these data, we use the full eq 9 with eq 12 (κ = 1) which yields[33,35a]

$$k_{qc} = \frac{K_{12}\nu_{23} \exp(-\Delta G^*_{23}/RT)}{1 + \nu_{23} \exp((\Delta G°_{23} - \Delta G^*_{23})/RT)/(k_{30} + k_{34})} \quad (14)$$

Here, as before, k_{qc} is the value of the quenching rate constant corrected for the diffusion limit (k_{diff} = 2.0 × 10^9 M^{-1} s^{-1}) and k_{30} is the first-order rate constant for "back-reaction" of RuL$_3^{3+}$ and RhL$_3^{2+}$. In view of the results on the bipyridinium system, k_{30} is assumed to be driving-force independent in this system as well; it is calculated as 1.7 × 10^{10} s^{-1} from the cage escape yield for the Rh(bpy)$_3^{3+}$–*Ru(bpy)$_3^{2+}$ reaction (0.15)[27] and k_{34} (3 × 10^9 s^{-1}). The frequency ν_{23} is taken as 1 × 10^{13} s^{-1} and K_{12} as 0.7 M^{-1}. The solid curve in Figure 3 was calculated from eq 14 with the above parameters together with $E°_{Q,Q^-}$ = −0.97 V and $k_{11}k_{22}$ = 5.25 × 10^{18} M^{-2} s^{-2} (ΔG^*_0 = 0.209 eV). The fit is quite acceptable and strongly supports the model involving endergonic and facile electron transfer for the *RuL$_3^{2+}$–Rh(4,4'-(CH$_3$)$_2$bpy)$_3^{3+}$ reactions.

In Figure 4 are shown data for other rhodium(III) complexes. None of these complexes exhibits a region of extremely steep free-energy dependence as was seen for the 4,4'-(CH$_3$)$_2$bpy complex. The experimental data are, however, consistent with eq 14 and $k_{11}k_{22}$, k_{30}, and ν_{23} as above if $E°_{Q,Q^-}$ for the 5,6-(CH$_3$)$_2$phen, 5-(CH$_3$)phen, and bpy complexes are −0.89, −0.88 and −0.86 V, respectively, and the curves shown in Figure 4 were calculated by using these parameters. The data reported for Rh(phen)$_3^{3+}$ in ref 27 are consistent with $E°_{Q,Q^-} \approx -0.84$ V (but k_{diff} = 1.6 × 10^9 M^{-1} s^{-1} in 0.5 M sulfuric acid). Although the errors are relatively large for these rhodium(III) systems because $k_q \approx k_{diff}$, it is nevertheless clear that these complexes react more rapidly with a given *RuL$_3^{2+}$ than does Rh[4,4'-(CH$_3$)$_2$bpy]$_3^{3+}$ (see also Table IV). This is the reason why a less negative $E°$ is required for these complexes.

As mentioned earlier, the electrochemical reduction of RhL$_3^{3+}$ is irreversible in water. Thus $E°_{Q/Q^-}$ cannot be directly measured for RhL$_3^{3+}$ = Q under the quenching conditions. A very striking result is however obtained when the values of $E°_{Q/Q^-}$ implicated by the quenching data are compared with $E_{1/2}$ values measured for the RhL$_3^{3+}$–RhL$_3^{2+}$ couples in acetonitrile. As shown in Table VII, for the five complexes for which the comparison can be made, E_{Q-Q^-} vs. SHE in water is 40–70 mV more negative than $E_{1/2}$ determined in acetonitrile vs. SCE. This is quite similar to the numerical difference noted for RuL$_3^{3+}$–RuL$_3^{2+}$ couples: $E_{1/2}$ values measured for the latter in water vs. SHE are 30 mV more
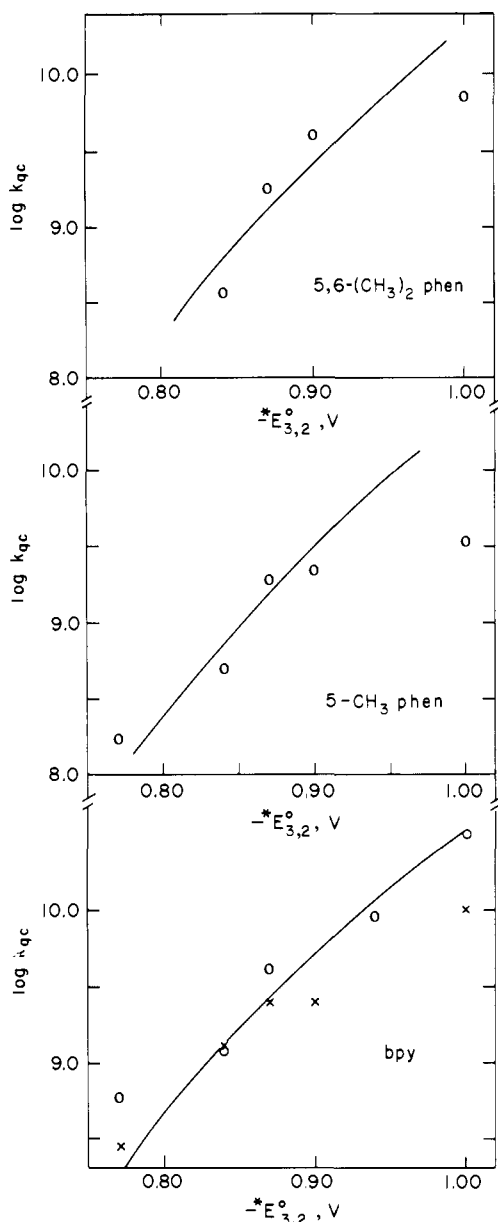
Poly(pyridine)ruthenium Redox Reactions

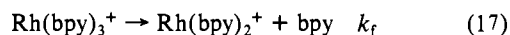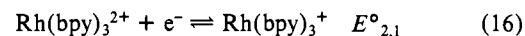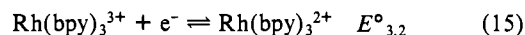J. Am. Chem. Soc., Vol. 104, No. 13, 1982 3625

Figure 4. The logarithm of the diffusion-corrected rate constant for the quenching of $*RuL_3^{2+}$ emission by RhL_3^{3+} vs. the reduction potential for the RuL_3^{3+}–$*RuL_3^{2+}$ couple. Parameters used as for Figure 3, except as noted: top, $Rh[5,6-(CH_3)_2phen]_3^{3+}$ ($E°_{Q,Q^-} = -0.89$ V); center, $Rh[5-(CH_3)phen]_3^{3+}$ ($E°_{Q,Q^-} = -0.88$ V); bottom, $Rh(bpy)_3^{3+}$ ($E°_{Q,Q^-} = -0.86$ V), circles for 0.5 M H_2SO_4 (ref 27, diffusion rate constant 1.3×10^9 M^{-1} s^{-1}), crosses for 0.17 M Na_2SO_4 (this work, diffusion rate constant 1.0×10^9 M^{-1} s^{-1}).

negative than those measured in acetonitrile relative to aqueous SCE.[5] This agreement substantiates the above k_q analysis and suggests further than $E_{1/2}$ values determined for the rhodium couples in acetonitrile can be used to estimate the RhL_3^{3+}–RhL_3^{2+} reduction potentials in aqueous solution.

The results obtained in the present study permit a clarification of the model for the RhL_3^{3+} cyclic voltammetric behavior observed in water. Previously[27] the irreversibility seen for $Rh(bpy)_3^{3+}$ was ascribed to a rapid reaction of the one-electron reduction product $Rh(bpy)_3^{2+}$ (an EC mechanism[39,40]). This description was based on an "absolute" current estimate in which the current due to the oxidation of $Ru(bpy)_3^{2+}$ was used as a reference.[27] We failed to appreciate that the diffusion coefficients for $M(bpy)_3^{2+}$ and $M(bpy)_3^{3+}$ could differ considerably; those for $Fe(phen)_3^{2+}$ and

$Fe(phen)_3^{3+}$ differ by a factor of 2.[41] Here we have redetermined the magnitude of the reduction current at E_{pc} in aqueous solution using $Cr(bpy)_3^{3+}$, rather than $Ru(bpy)_3^{2+}$, as standard; $Cr(bpy)_3^{3+}$ seems more appropriate as a reference because it is of the same charge as $Rh(bpy)_3^{3+}$ and its reduction occurs at a potential (-0.3 V vs. SHE) more similar to the potential for reduction of $Rh(bpy)_3^{3+}$ than that for oxidation of $Ru(bpy)_3^{2+}$ ($+1.3$ V). We find that the current for reduction of $Rh(bpy)_3^{3+}$ is 2.7 ± 0.2 times greater than that for $Cr(bpy)_3^{3+}$ under identical conditions. Thus the cathodic peak does not correspond to a one-electron change;[39,40] in fact $n \geq 1.8$. (Exact evaluation is not possible without more detailed knowledge of the system.[39,40]) We now conclude that, as is seen in acetonitrile at slow sweep rates,[30] rapid loss of bpy from $Rh(bpy)_3^+$ is responsible for the "irreversibility" of the $Rh(bpy)_3^{3+}$–$Rh(bpy)_3^{2+}$ couple in water at all sweeps (an EEC mechanism), i.e., eq 15–17. The reduction peak observed in water

$$Rh(bpy)_3^{3+} + e^- \rightleftharpoons Rh(bpy)_3^{2+} \quad E°_{3,2} \quad (15)$$

$$Rh(bpy)_3^{2+} + e^- \rightleftharpoons Rh(bpy)_3^+ \quad E°_{2,1} \quad (16)$$

$$Rh(bpy)_3^+ \rightarrow Rh(bpy)_2^+ + bpy \quad k_f \quad (17)$$

occurs near $E°_{3,2}$. Although $E°_{2,1}$ lies negative of $E°_{3,2}$, rapid reduction of $Rh(bpy)_3^{2+}$ does occur because k_f is very large. An analogous description has been proposed to account for the behavior observed at slow sweep rates in acetonitrile.[30] This mechanism provides a consistent model for other observations on the aqueous system: first, it accounts for the fact that the only oxidation wave seen in water (even at sweep rates as great as 100 V s^{-1} [27,42,43]) is that due to oxidation of Rh(I). Furthermore, no rapid additional reaction of $Rh(bpy)_3^{2+}$ is required—a very gratifying feature indeed, since none is detected spectrophotometrically in pulse radiolysis experiments.[44] In addition, the rapid loss of bpy required from $Rh(bpy)_3^+$ is consistent with the behavior seen in acetonitrile[30] (no anodic component to peak II was detected at $v \leq 50$ V s^{-1}) and with the preliminary estimate that k_f, the rate constant for eq 17, is $\sim 5 \times 10^4$ s^{-1} at 25 °C in water.[44] In discussing the proposed mechanism, we have focussed on $Rh(bpy)_3^{3+}$ because its fate upon reduction is better characterized than that of other RhL_3^{3+} complexes. It does, however, seem likely that the overall features of eq 15–17 also apply to the other RhL_3^{3+} systems in aqueous solution, although the detailed cyclic voltammetric parameters may change with L owing to changes in the value of $(E°_{3,2} - E°_{2,1})$ and to variations in the rate constant for loss of L from RhL_3^{3+}.

Flash photolysis of $Ru(bpy)_3^{2+}$–$Rh(bpy)_3^{3+}$ solutions has shown that $Ru(bpy)_3^{3+}$ and a "colorless" $Rh(bpy)_3^{2+}$ ($\epsilon \leq 10^3$ M^{-1} cm^{-1} in the visible region) result from the $*Ru(bpy)_3^{2+}$ quenching.[27] Similarly, pulse-radiolysis studies of $Rh(bpy)_3^{3+}$ have shown that the product of the reduction of $Rh(bpy)_3^{3+}$ by e_{aq}^- is (after >1 μs) a species which absorbs strongly in the ultraviolet region but negligibly in the visible.[27,45] This species has been described as a rhodium(II) complex $Rh(bpy)_3^{2+}$. The alternative formulation of the reduction product as $Rh^{III}(bpy)_2(bpy^-)$ was rejected because this complex, like $*Ru(bpy)_3^{2+}$, $Ru(bpy)_3^+$, and other bound bipyridine radical ions,[6,46] should absorb strongly in the visible or near-UV region of the spectrum. We resurrect these considerations at this time because the quenching data observed for the RhL_3^{3+} complexes do not appear consistent with rate-determining formation of $Rh^{II}L_3^{2+}$. Rather, the large $k_{11}k_{22}$ required to fit the data implicates $Rh^{III}L_2(L^-)^{2+}$ as the immediate quenching product in these systems. The $k_{11}k_{22}$ value of 5.3×10^{18} M^{-2} s^{-2} requires an "average" exchange rate constant of $\sim 2 \times 10^9$ M^{-1} s^{-1} for both the $*RuL_3^{2+}$–RuL_3^{3+} and RhL_3^{2+}–RhL_3^{3+} couples.

(39) Bard, A. J.; Faulkner, L. R. "Electrochemical Methods: Fundamentals and Applications"; Wiley: New York, 1980.
(40) Nicholson, R. S.; Shain, I. *Anal. Chem.* **1964**, *36*, 706.

(41) Ruff, I.; Zimonyi, M. *Electrochim. Acta* **1973**, *18*, 515.
(42) Matsubara, T., unpublished work.
(43) Creutz, C.; Keller, A. D.; Schwarz, H. A.; Sutin, N. *ACS Symp. Ser.*, in press.
(44) Schwarz, H. A., unpublished work.
(45) Mulazzani, Q. G.; Emmi, S.; Hoffman, M. Z.; Venturi, M. *J. Am. Chem. Soc.* **1981**, *103*, 3362.
(46) The spectrum of $Ir^{III}(bpy)_2(bpy)H_2O^{2+}$ in which bpy is the reduction site features absorption maxima at 440–450 nm ($\epsilon \sim 2 \times 10^3$ M^{-1} cm^{-1}) and 395 nm ($\epsilon \sim 10^4$ M^{-1} cm^{-1}). Finlayson, M.; Watts, R., work in progress.

Such a high value is consistent with estimates for the $*RuL_3^{2+}-RuL_3^{3+}$ couple and reflects the small inner-sphere electron-transfer barrier for bpy$^-$–bpy couples and the small solvent reorganization barrier for $M(bpy)_3^{2+/3+}$ couples.[47] The same factors apply for the related $[Rh^{III}L_2(L^-)]^{2+}-Rh^{III}L_3^{3+}$ couples. By contrast, d^7–d^6 rhodium(II)–rhodium(III) couples should experience substantial inner-sphere barriers owing to the differing population of the metal e_g orbitals in the two oxidation states. Consequently, k_{22} for the $Rh^{II}L_3^{2+}-Rh^{III}L_3^{3+}$ exchange should be $\ll 2 \times 10^9$ M^{-1} s^{-1}. In fact, the analogous first-transition-series couple $(t_{2g})^6(e_g)^1$ $Co(terpy)_2^{2+}-(t_{2g})^6(e_g)^0$ $Co(terpy)_2^{3+}$ undergoes electron exchange with a rate constant of 1.9×10^3 M^{-1} s^{-1}.[48] In further support of the description of RhL_3^{2+} as $[Rh^{III}L_2(L^-)]^{2+}$ are the potentials estimated in Table VII for the $RhL_3^{3+}-RhL_3^{2+}$ couples. At the far right of the table are values for the $RuL_3^{3+}-*RuL_3^{2+}$ ($Ru^{III}L_3^{3+}-[Ru^{III}L_2(L^-)]^{2+}$) couples. The similarities in the magnitudes of the potentials for a given ligand are remarkable but are expected when RhL_3^{2+} is formulated as $[Rh^{III}L_2(L^-)]^{2+}$ because the L–L$^-$ potential is largely sensitive only to the charge of the metal to which L is bound.[49]

In summary, the quenching studies in aqueous solution and the cyclic voltammetric experiments in acetonitrile have made possible the elucidation of the redox properties of the $RhL_3^{3+}-RhL_3^{2+}$ couple. In water at 25 °C (0.5 M ionic strength) the self-exchange rate for the couple is $>10^9$ M^{-1} s^{-1}. The reduction potential is a function of L and lies in the range -0.7 to -1.0 V vs. SHE. These properties strongly suggest the description of the reduced species as $[Rh^{III}L_2(L^-)]^{2+}$, but, as mentioned earlier, the spectrum observed for RhL_3^{2+}, at least when L = bpy of 4,4'-$(CH_3)_2bpy$,[44] is not characteristic of bound L$^-$. In addition, the substitution reactivity of RhL_3^{2+} is more characteristic of a rhodium(II) than a rhodium(III) metal center. The anomalous nature of RhL_3^{2+} is discussed in greater detail elsewhere[43] and will be the focus of future work.

Osmium Ammines. Plots of the logarithm of k_q (Table V) vs. $*E^\circ_{3,2}$ for the $RuL_3^{3+}-*RuL_3^{2+}$ couple are shown at the top of Figure 5 for $Os(NH_3)_5I^{2+}$, $Os(NH_3)_5Cl^{2+}$, $Os(NH_3)_6^{3+}$, and $Os(NH_3)_5H_2O^{3+}$ as quenchers. It is apparent that the quenching rate constants increase with the reducing power of $*RuL_3^{2+}$, i.e., k_q increases as $*E^\circ_{3,2}$ becomes more negative. In itself this is the rate trend expected for oxidative quenching of $*RuL_3^{2+}$ (eq 2) rather than for reductive quenching (eq 3) or energy transfer (eq 1). However the initial slopes of the plots for these three quenchers are much less than the theoretical value of 8.5 V^{-1}. (Since the quenching rate constants, except for $Os(NH_3)_5I^{2+}$, are $\ll 10^9$ M^{-1} s^{-1} no correction for diffusion is required.) From the E° data in Table V oxidative quenching is thermodynamically favorable for all of the $Os(NH_3)_6^{3+}$ and $Os(NH_3)_5H_2O^{3+}$ systems and for two of the four $Os(NH_3)_5Cl^{2+}$ systems. Since the driving force is moderate for all of these systems the very weak dependence of log k_q on $*E^\circ_{3,2}$ is informative. As the behavior of $Os(NH_3)_5I^{2+}$ is the most extreme it is discussed first.

The magnitudes of the quenching rate constants for $Os(NH_3)_5I^{2+}$ suggest that the quenching mechanism involves more than eq 2. The k_q values of 10^8–10^9 M^{-1} s^{-1} for K values near unity (for eq 2) would require the geometric mean of the self-exchange rates of the osmium(III)–osmium(II) couple and the $RuL_3^{3+}-*RuL_3^{2+}$ couple to be $\geq 10^8$ M^{-1} s^{-1} thus requiring the self-exchange rate for the $Os(NH_3)_5I^{2+}-Os(NH_3)_5I^+$ couple to be $\sim 10^7$ M^{-1} s^{-1}. The latter value seems unreasonably high in view of the fact that the self-exchange rates for the related ruthenium couple $Ru(NH_3)_6^{3+}-Ru(NH_3)_6^{2+}$ is $<10^5$ M^{-1} s^{-1}.[50] Furthermore, although k_q does increase somewhat with the reducing power of $*RuL_3^{2+}$, a rate variation of less than a factor of 3 is found. Thus it is likely that eq 1 and/or eq 3 also contribute to the observed quenching rate constant. Quenching by free iodide ion (eq 3) is "slow"; k_q is less than 10^5 M^{-1} s^{-1}. The complex

(47) Brown, G. M.; Sutin, N. *J. Am. Chem. Soc.* **1979**, *101*, 883.
(48) Cummins, D.; Gray, H. B. *J. Am. Chem. Soc.* **1977**, *99*, 5158.
(49) Creutz, C. *Comments Inorg. Chem.* **1982**, *1*, 293.
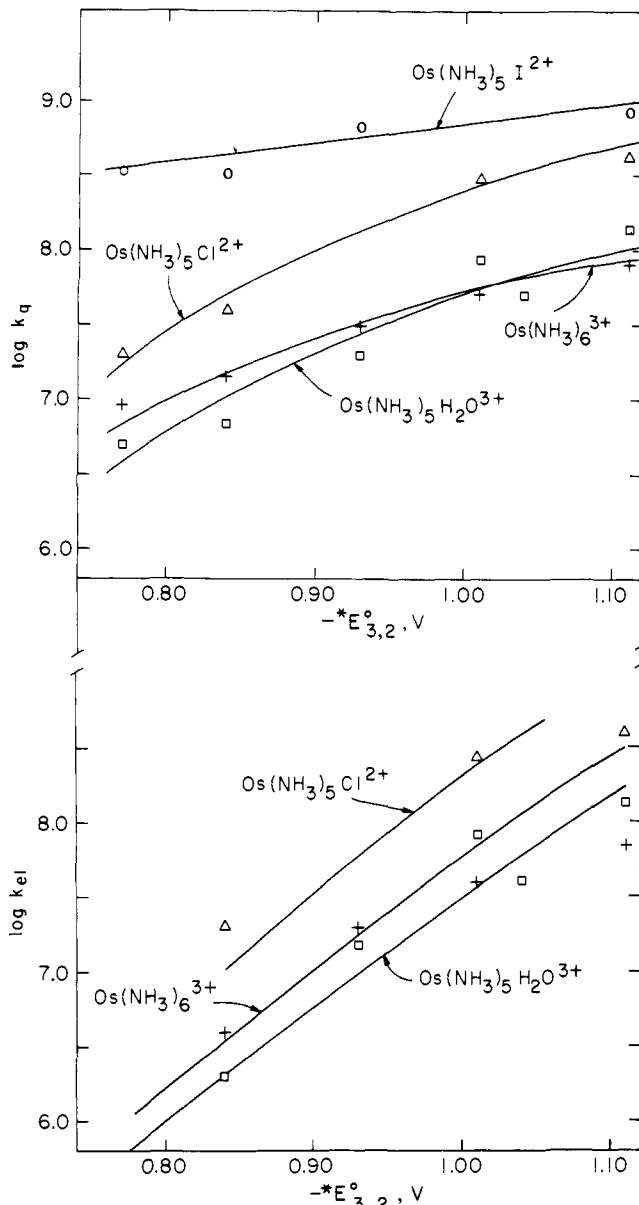(50) Meyer, T. J.; Taube, H. *Inorg. Chem.* **1968**, *7*, 2369.

Figure 5. Top: the logarithm of the rate constant for the quenching of $*RuL_3^{2+}$ emission by osmium(III) ammines vs. the reduction potential for the $RuL_3^{3+}-*RuL_3^{2+}$ couple. Bottom: the logarithm of the rate constant for oxidative quenching ($k_{el} = k_q - k_{en}$, see text) vs. the excited-state reduction potential.

$Os(bpy)_3^{3+}$ ($E^\circ = +0.82$ V) is reduced by $Os(NH_3)_5I^{2+}$ in 0.5 M H_2SO_4, but the rate constant is so small ($<10^2$ M^{-1} s^{-1}) that it can be anticipated that reduction of $*Ru(bpy)_3^{2+}$ ($E^\circ = +0.84$ V) will not be a major quenching pathway. This conclusion is supported by the observations of Buhr, Winkler, and Taube,[16] who find that none of the pentaammineosmium(III) complexes considered here is oxidized electrochemically at less than $+0.97$ V. These considerations suggest that $Os(NH_3)_5I^{2+}$ quenches predominantly by an energy-transfer pathway. From the magnitude of k_q for $Ru[5-(Cl)phen]_3^{2+}$, the rate constant k_{en} for the energy transfer pathway is estimated as 3×10^8 M^{-1} s^{-1}. Such a large energy-transfer rate constant suggests that energy transfer from the $\sim 17 \times 10^3$ cm^{-1} RuL_3^{2+} excited states to an acceptor state on $Os(NH_3)_5I^{2+}$ is not too unfavorable. Iodopentaammineosmium(III) manifests LMCT absorption at 24.5×10^3 cm^{-1}[51] and near-infrared absorption at 4.0×10^3 cm^{-1} attributed to vibrationally coupled metal-centered intraconfigurational transitions.[16] The osmium(III) acceptor state relevant to the quenching could be the LMCT state if the latter is considerably distorted.

(51) Verdonck, E.; Vanquickenborne, L. G. *Inorg. Chem.* **1974**, *13*, 762.

Another possibility is that "the" LMCT state is a manifold of spin–orbit coupled states with only one of the higher energy components being detected spectroscopically. The energy transfer from *RuL$_3^{2+}$ might populate one of the lower energy components.

The operation of an energy transfer pathway with Os(NH$_3$)$_5$I^{2+} suggests an explanation for the weak free-energy dependence seen for the other osmium(III) quenchers in Figure 5. If it is assumed that k_q for the poorest reductant *Ru[5-(Cl)phen]$_3^{2+}$ is due entirely to the energy-transfer pathway, the other quenching rate constants ($k_q = k_{en} + k_{el}$) may be broken up into energy transfer (k_{en}) and oxidative electron transfer (k_{el}) components. Thus k_{en} is 0.05 × 10^8, 0.1 × 10^8, and 0.2 × 10^8 M^{-1} s^{-1} for Os-(NH$_3$)$_5$H$_2$O^{3+}, Os(NH$_3$)$_6^{3+}$, and Os(NH$_3$)$_5$Cl^{2+}, respectively. At the bottom of Figure 5 the logarithms of the values of k_{el} obtained in this fashion have been plotted against *$E°_{3,2}$. It is apparent that the predicted free energy dependence is now observed. The curves shown were calculated from eq 10–13 ($K\nu = 1 \times 10^{12}$ M^{-1} s^{-1}), the $E°$'s in Table V, and log ($k_{11}k_{22}$) values of 10.8, 12.1, and 14.2 for Os(NH$_3$)$_5$H$_2$O^{3+}, Os(NH$_3$)$_6^{3+}$, and Os(NH$_3$)$_5$Cl^{2+}, respectively. The latter composite exchange parameters implicate exchange rate constants of ~10^2, 10^3, and 10^5 M^{-1} s^{-1} for the Os(NH$_3$)$_5$H$_2$O$^{3+/2+}$, Os(NH$_3$)$_6^{3+/2+}$, and Os(NH$_3$)$_5$Cl$^{2+/+}$ couples, respectively. These are of the order seen for ruthenium ammine couples. Interestingly, while the exchange rate for Ru-(NH$_3$)$_5$Cl$^{2+/+}$ has not been evaluated, its reactivity toward outer-sphere reductants is (like Os(NH$_3$)$_5$Cl^{2+}) greater than that of the corresponding aquo pentaammine and hexaammine complexes.[52,53] As mentioned earlier, no redox products were detected in the quenching of *RuL$_3^{2+}$ by osmium(III) complexes. The limit on the cage escape yields for these systems (Scheme I) is thus <0.05. If $k_{34} \approx 10^9$ M^{-1} s^{-1}, k_{30} for oxidation of osmium(II) by RuL$_3^{3+}$ is >2 × 10^{10} s^{-1}.

In contrast to the behavior of these osmium(III) complexes, the quenching rate constants for the osmium(II) complex Os-(NH$_3$)$_5$N$_2^{2+}$ increase with the oxidizing power of *RuL$_3^{2+}$ (i.e., with *$E°_{2,1}$). This is indicative of reductive quenching, which, in light of the value of the Os(NH$_3$)$_5$N$_2^{3+}$–Os(NH$_3$)$_5$N$_2^{2+}$ potential (+0.56 V)[54] is thermodynamically favorable for all the RuL$_3^{2+}$ complexes examined. The magnitude of the quenching rate constants suggests a self-exchange rate constant of the order of 10^3 M^{-1} s^{-1} for the Os(NH$_3$)$_5$N$_2^{3+}$–Os(NH$_3$)$_5$N$_2^{2+}$ couple.

The transient observed on reaction of Os(NH$_3$)$_5$Cl^{2+} with e$_{aq}^-$ or H atoms has absorption maxima at ~305 and 360 nm. Although the high $G\epsilon$ values (>10^3 M^{-1} cm^{-1}) are not consistent with assignment of the bands to pure ligand field (LF) transitions on osmium(II), the spectrum may be due to overlapping charge-transfer and LF absorption as is seen for ruthenium(II) ammines.[55-57] The very large rate constant ($k \approx 5 \times 10^9$ M^{-1} s^{-1})

for reaction of Os(NH$_3$)$_5$Cl^{2+} with H atoms observed in the present study may be compared with those for cobalt and ruthenium ammines which lie in the range 10^6–10^9 M^{-1} s^{-1}.[58,59] It is similar to that for Co(NH$_3$)$_5$I^{2+}.[57] While the pulse radiolysis and flash photolysis implicate formation and protonation of Os(NH$_3$)$_5$Cl$^+$, the continuous radiolysis and photolysis experiments show that reduction of water by Os(NH$_3$)$_5$Cl$^+$ and Os(NH$_3$)$_5$Cl(H)$^{2+}$ does not compete with reformation of Os(NH$_3$)$_5$Cl^{2+} by other routes. These routes have not been elucidated but presumably involve reaction with oxidizing species such as the *tert*-butyl alcohol radical, O$_2$, and H$_2$O$_2$ in the continuous-radiolysis experiments and Eu^{3+}, ascorbate radical, and dehydroascorbic acid in the continuous photolysis experiments. Although the reactions of Os(NH$_3$)$_5$Cl$^+$ and Os(NH$_3$)$_5$Cl(H)$^{2+}$ are incompletely characterized, it is evident that our results are not in accord with those of electrochemical studies. Pseudo-first-order rate constants ranging from 0.3 × 10^3 to 1.9 × 10^3 s^{-1} (pH 5.8 and 4.8, respectively) were extracted for the reaction of electrogenerated Os(NH$_3$)$_5$Cl$^+$ with H$^+$.[13,14] Under our conditions, the reaction of Os(NH$_3$)$_5$Cl$^+$ with H$^+$ is much slower ($k_{obsd} \approx 5.5 \times 10^2$ s^{-1} at pH 2) and, furthermore, does not yield much (if any) H$_2$. Further studies are required to resolve this inconsistency.

Conclusions

In this study the series of RuL$_3^{2+}$ excited states has been used to generate the one-electron reduction products of bipyridinium cations, Rh^{III}L$_3^{3+}$ complexes, and Os^{III}(NH$_3$)$_5$X^{2+} derivatives. The established redox properties of the *RuL$_3^{2+}$–RuL$_3^{3+}$ couples along with the preequilibrium Marcus formalism have been used to characterize these couples. For the bipyridinium cation and osmium ammine couples the work has led to self-exchange rate constant estimates of (0.5–2.0) × 10^6 and 10^2–10^5 M^{-1} s^{-1}, respectively, at 25 °C and 0.5 M ionic strength. For the Rh^{III}L$_3^{3+}$ complexes, the quenching studies, along with electrochemical experiments in acetonitrile, have permitted the estimation of both reduction potentials (−0.7 to −1.0 V vs. SHE depending upon L) and self-exchange rate constants (~2 × 10^9 M^{-1} s^{-1}) for the RhL$_3^{3+}$–RhL$_3^{2+}$ couples in aqueous solution. The use of RuL$_3^{2+}$ excited states has thus proven quite powerful in elucidating the properties of highly reducing species.

Supplementary Material Available: Analytical results for RhL$_3$(ClO$_4$)$_3$ and ultraviolet spectra of RhL$_3^{3+}$ (2 pages). Ordering information is given on any current masthead page.

(52) Jacks, C. A.; Bennett, L. E. *Inorg. Chem.* **1974**, *13*, 2035.
(53) Stritar, J.; Taube, H. *Inorg. Chem.* **1969**, *8*, 2281.
(54) Buhr, J. D.; Taube, H. *Inorg. Chem.* **1980**, *19*, 2425.
(55) Lever, A. B. P. "Inorganic Electronic Spectroscopy"; Elsevier: New York, 1968; p 305.
(56) Matsubara, T.; Ford, P. C. *Inorg. Chem.* **1978**, *17*, 1747.
(57) The visible–UV absorption spectra of Ru(NH$_3$)$_6^{2+}$, Ru(en)$_3^{2+}$, and Ru(NH$_3$)$_5$H$_2$O^{2+} manifest a weak shoulder (370–415 nm, ϵ 30–120 M^{-1} cm^{-1}) and a higher intensity maximum (270–300 nm, ϵ 500–1000 M^{-1} cm^{-1}).[58] For Ru(NH$_3$)$_6^{2+}$, the 390-nm shoulder has been assigned to the ^{1}A$_{1g} \rightarrow {}^1$T$_{1g}$ LF transition;[59] the ^{1}A$_{1g} \rightarrow {}^1$T$_{2g}$ band has been observed at 310 nm. The intense higher energy bands (which may also overlap ligand field transitions) have been ascribed substantial charge-transfer character. For osmium(II), the LF bands should occur at somewhat higher energy than for Ru(II). Using the shift between the LF bands of 4d Rh(III) and 5d Ir(III), an energy increase of ~20% would be expected. Thus LF transitions in the vicinity of 300 nm are expected for Os(NH$_3$)$_6^{2+}$ and the Os(NH$_3$)$_5$Cl$^+$ absorption could be shifted to somewhat longer wavelength. The position of charge-transfer-to-solvent (CTTS) absorption for Os(NH$_3$)$_5$Cl$^+$ may be similarly estimated by taking into account the ~0.9 V greater oxidizability of Os(II) compared to Ru(II) and the CTTS absorption maximum for Ru(NH$_3$)$_6^{2+}$ in water (275 nm). Intense CTTS absorption for Os(NH$_3$)$_5$Cl$^+$ is thus predicted at ~330 nm. These considerations show that overlapping LF and CTTS absorptions with molar absorptivities on the order of 10^3 M^{-1} cm^{-1} might be expected at 300–330 nm for Os(NH$_3$)$_5$Cl$^+$ and the observed transient spectrum is consistent with these expectations.
(58) Navon, G.; Stein, G. *J. Phys. Chem.* **1965**, *69*, 1390.
(59) Navon, G.; Meyerstein, D. *J. Phys. Chem.* **1970**, *74*, 4067.